Divalent Rab effectors regulate the sub-compartmental organization and sorting of early endosomes

Stefano De Renzis*, Birte Sönnichsen† and Marino Zerial*‡

**Max Planck Institute for Molecular Cell Biology and Genetics, Pfotenhauerstrasse, 01307 Dresden, Germany*
†Cenix BioScience GmbH, Pfotenhauerstrasse, 01307 Dresden, Germany
‡e-mail: zerial@mpi-cbg.de

Published online: 14 January 2002, DOI: 10.1038/ncb744

The three GTPases Rab5, Rab4 and Rab11 regulate sequential transport steps along the endocytic/recycling pathway, and occupy distinct membrane domains on early and recycling endosomes. To address the mechanisms that regulate communication between such domains, we searched for proteins that interact with both Rab5 and Rab4. Here, we report that Rabenosyn-5, a previously identified Rab5 effector, also binds to Rab4. Rabenosyn-5 overexpression increased the association between Rab5 and Rab4 endosomal domains and decreased the fraction of Rab4- and Rab11-positive structures. This redistribution was accompanied by a faster rate of transferrin recycling from early endosomes to the cell surface and reduced transport to Rab11-containing perinuclear recycling endosomes. These effects depend on the ability of Rabenosyn-5 to interact with Rab4. We propose that divalent Rab effectors regulate protein sorting and recycling by connecting Rab domains on early endosomes.

Early endosomes are multifunctional organelles that regulate membrane transport between the plasma membrane and various intracellular compartments[1]. After arrival at early endosomes, endocytosed solutes, membrane proteins and lipids are either returned to the plasma membrane, as in the case of recycling receptors and bulk membrane constituents[2–4], or transported to late endosomes and lysosomes for degradation[5,6]. Another transport route connects early endosomes to the *trans*-Golgi network (TGN)[7,8]. Given that the early endosome functions as a transport node, its sorting and recycling activities are fundamental to proper cellular function and growth[5]. From this organelle, recycling components can return directly to the plasma membrane through a 'fast' recycling route[4,9], or can take a 'slow' recycling pathway through perinuclear recycling endosomes[3,10].

Despite a detailed morphological analysis of cargo transport through endosomal compartments, the molecular mechanisms underlying protein sorting and membrane recycling are largely unknown. Rab GTPases exert a regulatory function in both exocytic and endocytic transport, through the recruitment of specific effector proteins to the membrane on which they are localized[11,12]. Rab5 regulates the binding and recruitment of a large number of effector proteins to early endosomes[13]. Importantly, these molecules act cooperatively. The Rabaptin-5–Rabex-5 complex activates Rab5 (ref. 14), which can then bind to hVps34, a phosphatidylinositol-3-OH kinase[15] that specifically generates phosphatidyinositol-3-phosphate (PI(3)P)[16]. The concomitant presence of PI(3)P in the environment of active Rab5 is essential for the localization of two other Rab5 effectors, EEA1 (refs 13, 17) and Rabenosyn-5 (ref. 18), which both bind to PI(3)P through their FYVE finger domain and provide complementary regulatory functions on SNAP receptors (SNAREs)[13,18,19]. On the basis of localized lipid production and cooperativity between effectors and oligomerization, we have proposed that Rab5, through its effector proteins, organizes a membrane domain defining the site of entry into early endosomes[20,21]. Rab4 and Rab11, which are implicated in the fast and slow recycling pathway, respectively[22,23], are localized to separate membrane domains on early endosomes that are distinct from those harbouring Rab5 (ref. 20). These domains are arranged non-randomly, with three major endosomal populations, one containing mainly Rab5, a second both Rab5 and Rab4, and a third with mainly Rab4 and Rab11 (ref. 20).

The model of membrane compartmentalization of Rab proteins and their effectors helps us to understand the molecular basis of the structural and functional properties of early endosomes. First, the molecules that permit membranes to fuse with and recycle from early endosomes should not be randomly distributed, but arranged within defined membrane areas. This is consistent with the partitioning of early endosomes in morphologically distinct subcompartments, vesicles, cisternae and tubules[24,25]. Second, the molecular principles that lead to partitioning of the endosome membrane into different areas would ensure that little or no intermixing between domains occurs, despite the extensive transport of membranes through early endosomes. Third, although segregated, these domains should communicate with each other. Recycling receptors internalized from the surface first enter the Rab5 domain, rapidly fill the adjacent Rab4 tubular domain and then enter the Rab11 domain, where they reside for long periods[20]. Given that Rab effectors are recognized as membrane-tethering molecules[13,26–29], one possible point of regulation to link Rab domains would be at the level of these proteins. The finding that Rabaptin-5 also interacts with Rab4 through a distinct binding site[30] supports this idea. The aim of this work was to determine how the PI(3)P- and Rab5-dependent entry into sorting endosomes is linked to the sequential exit into the Rab4-positive domain. We have addressed this question by searching for effectors shared by Rab5 and Rab4.

Results

Identification of proteins that interact with both active Rab5 and Rab4. To identify Rab5 effectors that also interact with Rab4, we used an experimental strategy based on two sequential steps of affinity chromatography, the first to purify Rab5-interacting proteins and the second to absorb them onto glutathione *S*-transferase (GST)–Rab4. Glutathione beads containing GST–Rab5 loaded with

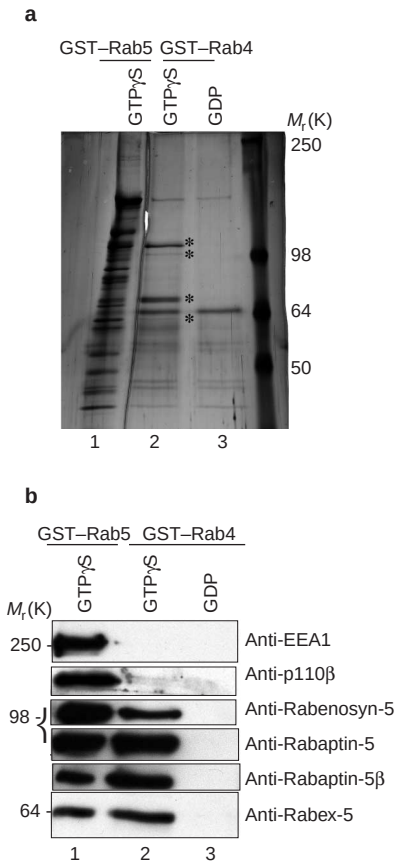

Figure 1 **Purification and identification of common effectors of Rab5 and Rab4 by sequential affinity chromatography. a**, GST–Rab5-GTPγS affinity columns were incubated with bovine brain cytosol. Bound proteins were eluted (lane 1), and subsequently incubated with GST–Rab4-GTPγS (lane 2) or GST–Rab4-GDP (lane 3). Bound proteins were eluted and analysed by gradient SDS–PAGE and silver staining. **b**, Western blot analysis of proteins that interact with both active Rab5 and Rab4 (lane 1, 2) or inactive Rab4 (lane 3) purified as in **a**. The four bands indicated with an asterisk (**a**, lane 2) reacted positively after detection with anti-Rabaptin-5, anti-Rabaptin-5β, anti-Rabex-5 and anti-Rabenosyn-5 antibodies.

GTPγS were incubated with bovine brain cytosol. Bound proteins were eluted and applied to the column containing GST–Rab4 in the presence of GTPγS, or as a control, GDP. Bound proteins were eluted from the beads and analysed by SDS–polyacrylamide gel electrophoresis (PAGE) and silver nitrate staining (Fig. 1a, b). Rabaptin-5 has already been shown to interact with both Rab5 and Rab4 (ref. 30). Therefore, three proteins were expected: Rabaptin-5, Rabaptin-5β and their binding partner Rabex-5 (ref. 14). Four bands, instead of three, were visible in the eluate from the Rab4-GTPγS (Fig 1a, lane 2) but not the Rab4-GDP column (Fig. 1a, lane 3). By a combination of mass spectrometry and western blot analysis, these bands were found to correspond to Rabaptin-5, Rabaptin-5β, Rabex-5, and the fourth band to Rabenosyn-5 (Fig. 1b, lane 2). The specificity of these interactions was validated by the observation that under the same experimental conditions, two of the most abundant Rab5 effectors, EEA1 (ref. 13) and p110β (ref. 15) did not interact with Rab4 (Fig. 1b, lanes 1,2).

Rabenosyn-5 was previously identified as a Rab5 effector regulating membrane tethering/fusion at the stage of entry into early endosomes[18]. Like EEA1, it is recruited to sorting endosomes in a Rab5- and PI(3)P-dependent manner, and both proteins colocalize within Rab5-positive endosomes[18]. The finding that Rabenosyn-5

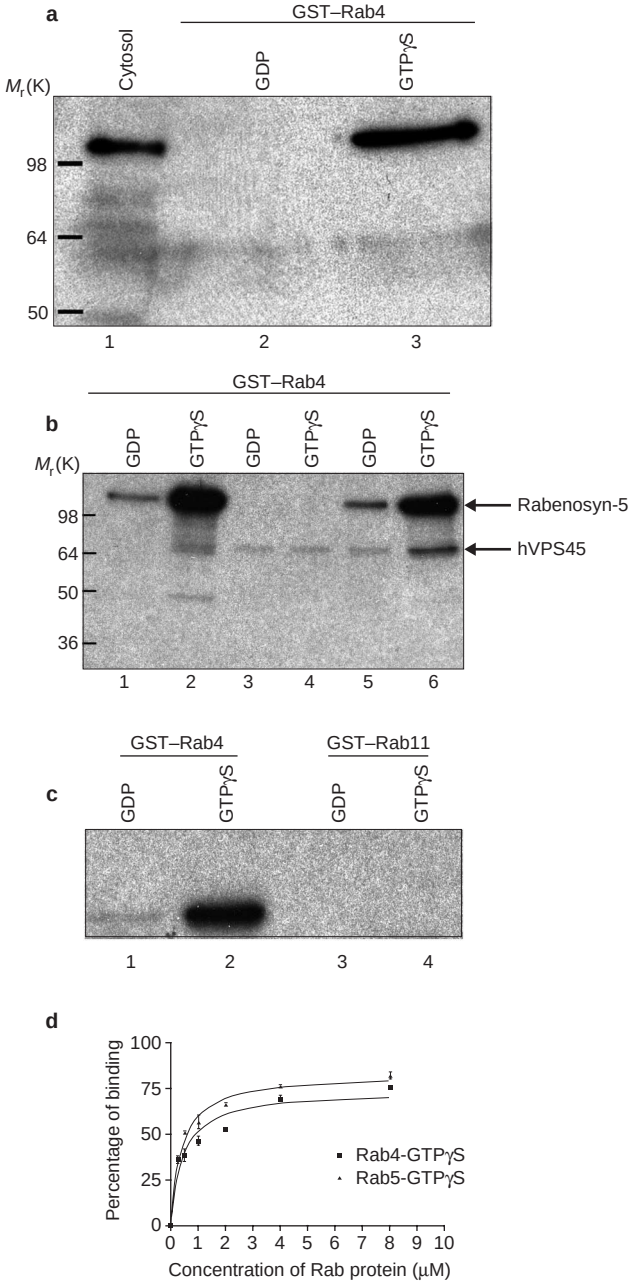

Figure 2 **Rabenosyn-5 interacts directly with Rab4 and recruits hVps45 to Rab4. a**, Cytosolic Rabenosyn-5 interacts with Rab4. Bovine brain cytosol (lane 1) was incubated with GST–Rab4-GDP (lane 2) or GST–Rab4-GTPγS (lane 3). Bound proteins were eluted, separated by SDS–PAGE and analysed by immunoblotting with antibodies against Rabenosyn-5. **b**, GST–Rab4-GDP (lanes 1, 3 and 5) or GST–Rab4-GTPγS (lanes 2, 4 and 6) were incubated with ^{35}S-methionine-labelled *in vitro* translated Rabenosyn-5 alone (lanes 1 and 2), hVps45 alone (lanes 3 and 4) or cotranslated Rabenosyn-5 and hVps45 (lanes 5 and 6, respectively). Bound proteins were eluted and analysed by SDS–PAGE and autoradiography. **c**, Rabenosyn-5 does not interact with Rab11. GST–Rab4-GDP (lane 1), GST–Rab4-GTPγs (lane 2), GST–Rab11-GDP (lane 3), GST–Rab11-GTPγs (lane 4), were incubated with ^{35}S-methionine-labelled *in vitro* translated Rabenosyn-5. Bound proteins were eluted and analysed as in **b**. **d**, Rabenosyn-5 has a similar affinity for Rab5 and Rab4. Rabenosyn-5 was *in vitro* transcribed and translated in the presence of ^{35}S-methionine and the percentage of binding to Rab5 and Rab4 was calculated, as described in the Methods.

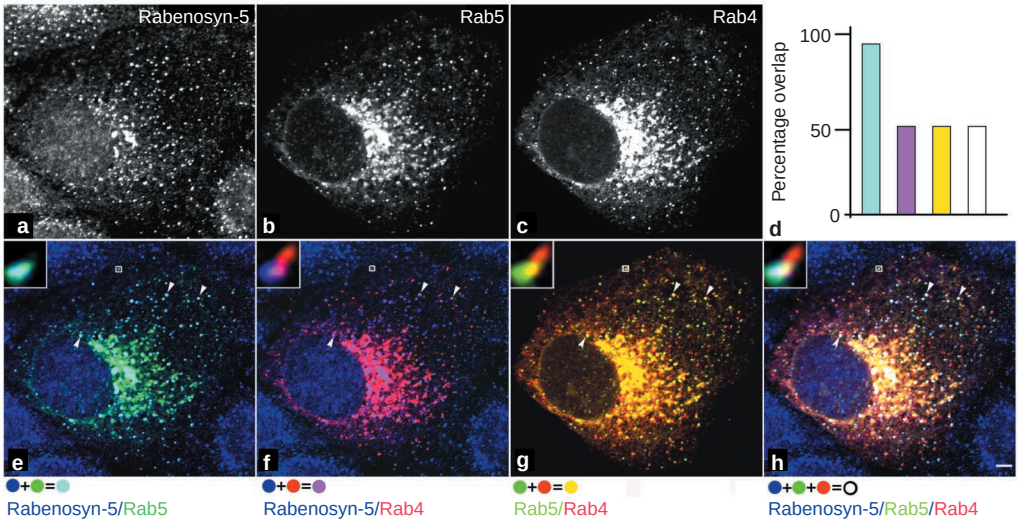

Figure 3 **Confocal immunofluorescence analysis of Rab5-, Rab4- and Rabenosyn-5-labelled endosomes.** A431 cells expressing CFP–Rab5 and YFP–Rab4 were fixed and stained with antibodies against Rabenosyn-5 and then with Texas-Red-conjugated secondary antibodies (panels **a**–**c** and **e**–**h**). Individual confocal sections are shown. Scale bar, 3μm. **d**, The extent of colocalization between Rab5, Rab4 and Rabenosyn-5 was quantified, as described in the Methods. Colours in the histogram correspond to the colours used to merge the double or triple fluorescent signals in the inset panels.

can also interact with Rab4 suggests an additional function for Rabenosyn-5 in early endosome function.

Biochemical characterization of the Rabenosyn-5–Rab4 interaction. To confirm that Rabenosyn-5 can interact with Rab4 independently of the pre-Rab5 purification step, GST–Rab4 was incubated directly with bovine brain cytosol and the bound proteins were analysed by western blot. Under these conditions, Rabenosyn-5 specifically interacted with Rab4-GTPγs (Fig. 2a, lane 3) but not with Rab4-GDP (Fig. 2a, lane 2).

In cytosol, Rabenosyn-5 is complexed with hVps45 (ref. 18), a Sec1-related protein that regulates the assembly of endosomal v- and t-SNAREs[31]. The interaction between Rab5 and Rabenosyn-5 is direct, whereas hVps45 interacts with Rab5 only through Rabenosyn-5 (ref. 18). To determine the pattern of interaction with Rab4, Rabenosyn-5 and hVps45 were either *in vitro* translated separately or cotranslated and incubated with glutathione beads containing GST–Rab4. Whereas Rabenosyn-5 interacted directly with Rab4 (Fig. 2b, lane 1,2), Vps45 did not bind Rab4, unless cotranslated with Rabenosyn-5 (Fig. 2b, compare lanes 3 and 4 with lanes 4 and 5). Thus, Rabenosyn-5 binds directly to Rab4 and, by analogy to Rab5; this interaction may serve as a link between Rab4 and Vps45.

The binding of Rabenosyn-5 to both Rab5 and Rab4 raises the question of whether Rabenosyn-5 also interacts with other Rab proteins. In particular, because of the association of the Rab4-positive domain with the Rab5-and Rab11-positive domain on early and recycling endosomes, we investigated whether Rab11 and Rabenosyn-5 also interact. Rabenosyn-5 neither interacts with Rab11 (Fig. 2c), nor with Rab2 and Rab33b, two Rab proteins associated with the biosynthetic pathway (data not shown).

Rabenosyn-5 is associated with endosomes where Rab5 and Rab4 colocalize. Rabenosyn-5 may influence the functional connection between Rab5 and Rab4 domains. Therefore, we investigated whether Rabenosyn-5 is localized to endosomes containing Rab5 alone, or both Rab5 and Rab4. To distinguish between these two possibilities, we used the same approach that previously visualized and quantified the distribution of Rab5, Rab4 and Rab11 on endosomes. This approach involves a combination of plasmid DNA microinjection, confocal microscopy and post-imaging processing[20]. Because of the lack of antibodies sensitive enough to detect endogenous Rab5 and Rab4, plasmids encoding GFP-tagged versions of these GTPases were microinjected into the cell nucleus. Compared with other transfection methods, this technique provides a lower and more reproducible level of expression of the Rab proteins, without detectable alterations in the morphology or the kinetics of transport through endocytic organelles[20].

A431 cells coexpressing cyan fluorescent protein (CFP)–Rab5 and yellow fluorescent protein (YFP)–Rab4 were fixed and stained with affinity-purified anti-Rabenosyn-5 antibodies. Confocal microscope serial sections were obtained and processed with deconvolution software before the overlapping fluorescent signal was quantified. The triple-labelling experiment shown in Fig. 3 indicates that 95% of Rabenosyn-5-positive endosomes also contained Rab5 (Fig. 3e), and of those, 55% were positive for Rab4 (Fig. 3f). Importantly, the latter pool corresponds to those endosomes positive for all three proteins (Fig. 3h). Therefore, whenever endosomes contained both Rab5 and Rab4, they were also positive for Rabenosyn-5 (arrows in Fig. 3e–h, and panel d for quantification). Interestingly, although Rab5 and Rabenosyn-5 always localized to the same endosomal domain, Rab4 was often segregated into elongated structures (Fig. 3, inset). These morphological data support the hypothesis that Rabenosyn-5 may regulate the functional link between Rab5- and Rab4-positive domains.

The localization of Rabenosyn-5 may reflect its higher affinity for Rab5 over Rab4, or could be a consequence of both Rab5- and PI(3)P-binding sites as a cooperative targeting determinant. We favour the latter possibility, as *in vitro* binding experiments established that Rab5 and Rab4 interact with Rabenosyn-5 with similar affinity (dissociation constant (K_d) ~350 nM; Fig. 2d). Moreover, as previously shown, the FYVE finger domain is necessary for the endosomal localization of Rabenosyn-5 (ref. 18) and, as with Rab4-positive endosomes, a substantial fraction of Rab5-positive structures (~40%) are devoid of Rabenosyn-5, indicating that Rab binding alone is insufficient to mediate Rabenosyn-5 recruitment to endosomal membranes.

Next, we determined whether Rab5 and Rab4 bind simultaneously to Rabenosyn-5, or whether binding is mutually exclusive. Rabenosyn-5 and hVps45 were coexpressed in insect cells with the

articles

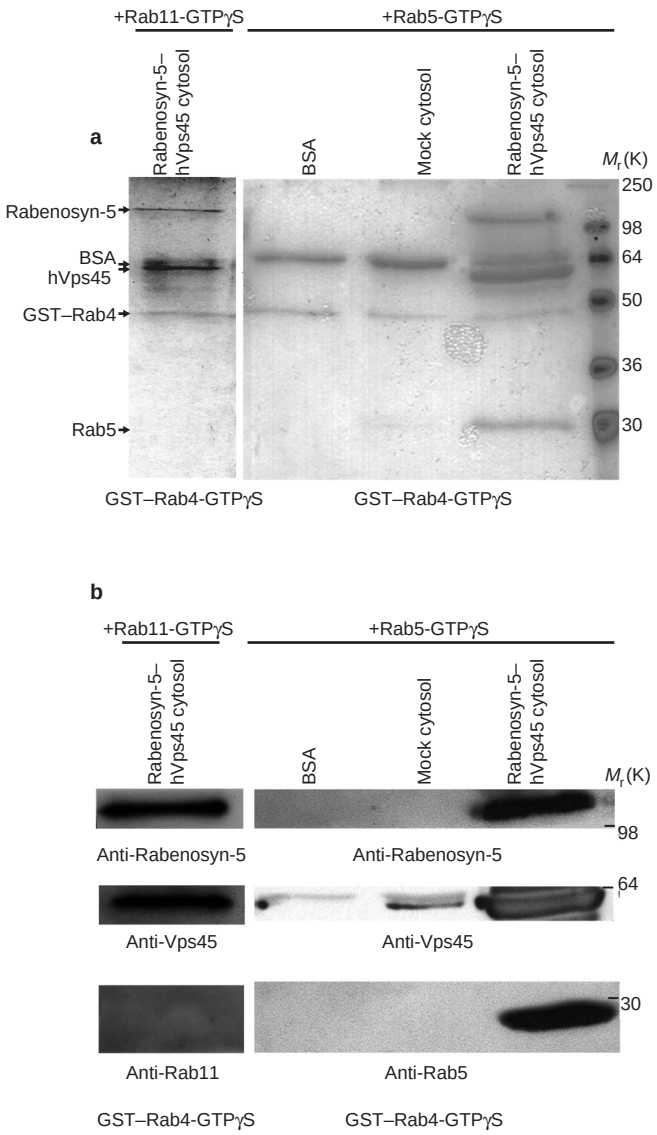

Figure 4 **Rabenosyn-5 binds simultaneously to Rab5 and Rab4. a**, GST–Rab4-GTPγS was incubated with cytosol containing overexpressed Rabenosyn-5–hVps45, mock-infected cytosol or BSA. After extensive washes, a second incubation was performed with purified Rab5-GTPγS and BSA or Rab11-GTPγS as a negative control. Bound proteins were eluted, separated by SDS–PAGE and transferred to nitrocellulose for Ponceau staining (**a**) or for western blot analysis (**b**).

Table 1 Quantification of Rab5, Rab4 and Rab11 overlap on the same endosomes.

	Rab5 + Rab4	Rab4 + Rab11	Rab5 + Rab4 +Rab11
Control	52 ± 4	50 ± 1	23 ± 2
+Rabenosyn-5	90 ± 6	17 ± 3	ND
+Rabenosyn-5 (δ264—500)	58 ± 5	ND	ND
+hVPS45	50 ± 3	ND	ND
+Rabenosyn-5 +hVPS45	92 ± 4	ND	ND
+Rabaptin-5	80 ± 3	ND	ND
+EEA1	60 ± 5	ND	ND

Fluorescence analysis: plasmids encoding the proteins indicated in the first column were microinjected in the nucleus of A431 cells. Numbers represent the percentage of endosomes labelled for the indicated combination of Rab proteins. ND, not determined.

baculovirus expression system. GST–Rab4 immobilized on Sepharose beads and loaded with GTPγS was incubated with cytosol containing overexpressed Rabenosyn-5 and hVps45 for 2 h. Unbound Rabenosyn-5–hVps45 complex was removed by washing and the GST–Rab4 column was further incubated with purified GTPγS-loaded Rab5, or with GTPγS-loaded Rab11 as a control. After extensive washes, bound proteins were eluted and analysed by western blotting and Ponceau S staining (Fig. 4). Rab5, but not Rab11, was recovered on the GST–Rab4 affinity column only when it had bound Rabenosyn-5–hVps45, but not if the pre-incubation was performed with either mock cytosol or BSA (Fig. 4a and b). These results indicate that Rab5 and Rab4 can bind simultaneously to Rabenosyn-5 *in vitro*.

Overexpression of Rabenosyn-5 increases the coupling between Rab5 and Rab4 domains. Under normal conditions, ~50% of early endosomes contain both Rab5 and Rab4 domains, whereas the remainder are segregated[20]. We examined whether the level of Rabenosyn-5 expression can influence this distribution. A431 cells were microinjected with plasmids encoding CFP–Rab5, YFP–Rab4 and Rabenosyn-5, and the number of endosomes containing both Rab5 and Rab4 was quantified as in Fig. 3. Overexpression of Rabenosyn-5 had two effects (Fig. 5a–c). First, it induced the formation of seemingly enlarged endosomal structures. Preliminary electron-microscopy studies suggest that these structures are not vacuolar, but retain a vaculotubular morphology (data not shown). Second, it drastically altered the segregation between Rab4 and Rab5 endosomes. Rab4 now almost completely colocalized with Rab5 and Rabenosyn-5 on the same endosomal structures (~90% versus ~55% in control; see also Table 1). This effect is not caused by a titration of endogenous hVps45, as coexpression of hVps45 and Rabenosyn-5 did not revert the phenotype observed after overexpression of the proteins (Table 1). Overexpression of hVps45 alone had no effect, indicating that the phenotype observed is caused specifically by Rabenosyn-5. Therefore, we tested whether overexpression of Rabaptin-5, which also interacts with both Rab5 and Rab4, could induce a redistribution of Rab5- and Rab4-positive structures. Indeed, a similar, albeit less potent phenotype was observed after overexpression of Rabaptin-5 (80% of Rab4 endosomes also contain Rab5 versus 52% in the control; Fig. 5d–f and Table 1). By contrast, overexpression of EEA1, which binds to PI(3)P and Rab5, but not to Rab4, caused a significant enlargement of the Rab5-positive compartment but failed to alter the distribution of Rab5 and Rab4 domains (Fig. 5g–i and Table 1). Therefore, the ability of Rab5 and Rab4 domains to cluster and/or fuse together seems to be restricted to proteins that bind directly to both Rab5 and Rab4.

To determine whether the Rabenosyn-5–Rab4 interaction is necessary to redistribute the Rab4-positive membranes, we engineered a Rabenosyn-5 mutant devoid of Rab4-binding site(s). To this aim, a series of Rabenosyn-5 truncation mutants were constructed and tested for their ability to interact with Rab5 and Rab4 (see Fig. 5j). The Rab4-binding site was mapped between amino acids 264 and 500, immediately downstream of the FYVE finger domain. This region shares no homology with Rabaptin-5 or Rabip4, another FYVE finger-containing protein recently identified as a Rab4 effector[32]. A Rab5-binding site was mapped to the extreme carboxy-terminal end of the protein, between amino acids 627 and 784. A low-affinity Rab5-binding activity was also found in the region encoding the Rab4-binding site. Therefore, we succeeded in generating a Rabenosyn-5 mutant (δ; amino acids 264–500) devoid of the Rab4-binding site, yet still capable of interacting with

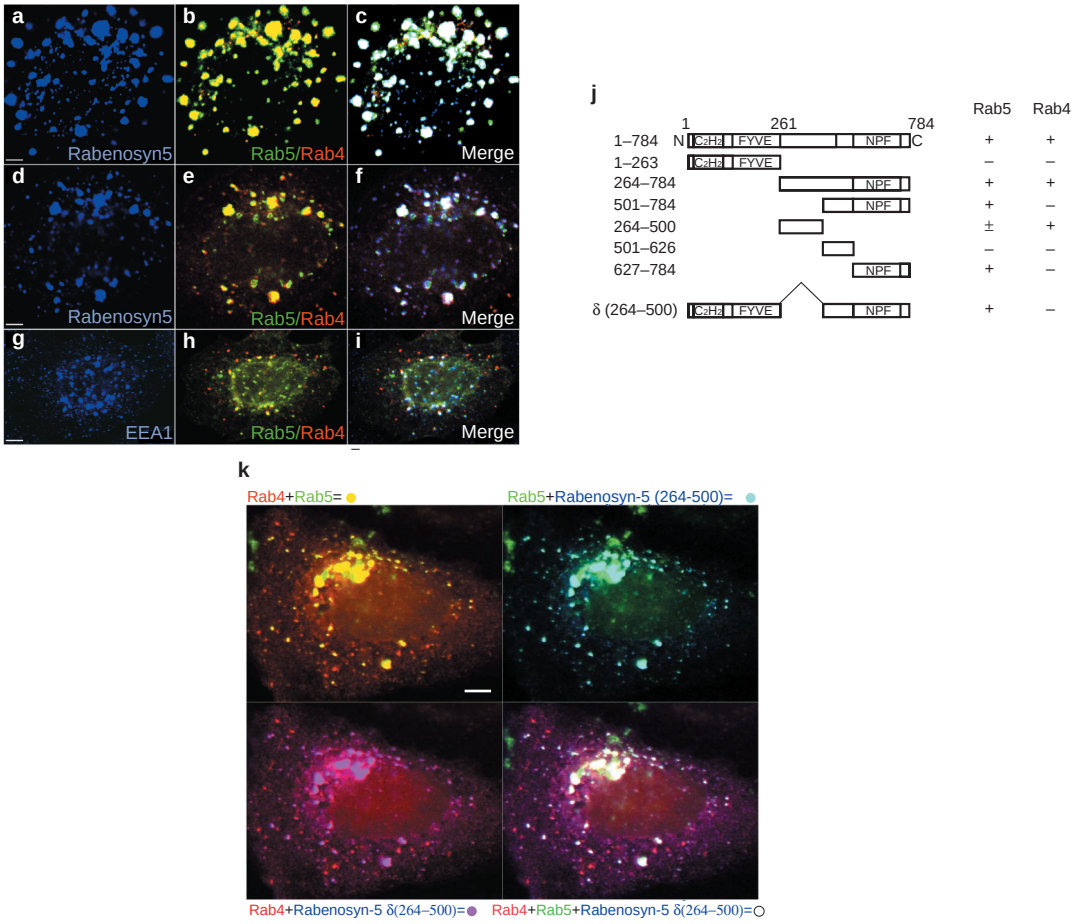

Figure 5 **Overexpression of Rabenosyn-5 and Rabaptin-5, but not EEA1, increases Rab5 and Rab4 colocalization. a–i**, Rabenosyn-5 (**a–c**), Rabaptin-5 (**d–f**) or EEA1 (**g–i**) was coexpressed with CFP–Rab5 and YFP–Rab4 in A431 cells. Cells were fixed and stained with antibodies against Rabenosyn-5 (**a–c**), Rabaptin-5 (**d–f**), and EEA1 (**g–i**). Individual confocal sections are shown. Scale bar, 4μm (**a–f**) and 5μm (**g–i**). **j**, *In vitro* binding assay to determine Rab4 and Rab5-binding sites on Rabenosyn-5. Full-length Rabenosyn-5, or truncation mutants thereof, were *in vitro* translated and binding to GST–Rab4 and GST–Rab5 estimated, as in Fig. 2. **k**, The Rabenosyn-5–Rab4 interaction is necessary for Rab4 endosomes to be redistributed. Myc-tagged Rabenosyn-5δ (residues 264–500) was coexpressed together with CFP–Rab5 and YFP–Rab4 in A431 cells. Cells were fixed and stained with antibodies against Myc. Individual confocal sections are shown. Scale bar 4μm.

Rab5 and PI(3)P. Rabenosyn-5δ completely colocalized with Rab5-positive endosomes, and like EEA1, it caused an apparent enlargement of these structures. However, this mutant protein failed to redistribute Rab4-positive endosomes (Fig. 5k and Table 1), suggesting that the activity of Rabenosyn-5 requires its interaction with Rab4. Binding to Rab4 is necessary, but not sufficient, to redistribute Rab4-positive endosomes. An overexpressed Rabenosyn-5 mutant lacking the FYVE finger (construct 264–784 in Fig. 5j), failed to localize to early endosomes and to redistribute Rab4 endosomes (data not shown). Therefore, both PI(3)P and Rab4 binding are necessary for Rabenosyn-5 to exert its effects.

Rabenosyn-5 does not interact with Rab11. If the effect of Rabenosyn-5 on the distribution of Rab5 and Rab4 domains is specific, the fraction of endosomes positive for both Rab5 and Rab11 domains should remain unaffected after Rabenosyn-5 overexpression. We consistently found that the typical perinuclear localization of Rab11-positive membranes was unaffected after Rabenosyn-5 overexpression (Fig. 6). Strikingly, concomitant with the increase in Rab5- and Rab4-positive endosomes, overexpression of Rabenosyn-5 reduced the proportion of endosomes labelled for both Rab4 and Rab11 (Table 1). In summary, overexpression of Rabenosyn-5 selectively shifted the distribution of Rab4 domains from the Rab4- and Rab11-positive endosomal populations to Rab5- and Rab4-positive endosomal populations.

Overexpression of Rabenosyn-5 stimulates transferrin recycling. Endocytosed transferrin is sequentially transported through Rab5, Rab4 and Rab11 endosomal domains before recycling back to the plasma membrane[20,23,33]. We tested whether the altered distribution of Rab-domains induced by Rabenosyn-5 affects the recycling of endocytic markers. Therefore, we analysed the transport of transferrin receptor through the endocytic and recycling pathway in cells overexpressing Rabenosyn-5. In control cells, after 15 min of continuous internalization, transferrin labelled peripheral small structures corresponding to early endosomes as well as perinuclear recycling endosomes (Fig. 7a). By contrast, in cells overexpressing Rabenosyn-5, transferrin accumulated in peripheral enlarged structures, but perinuclear recycling endosomes were poorly labelled (Fig. 7c–e, quantification in 7b).

It is unlikely that this effect is caused by a general block of exit from early endosomes, as transferrin was efficiently internalized. This implies that its receptor can cycle between endosomes and the plasma membrane. Instead, it is possible that transferrin is transported less efficiently to perinuclear recycling endosomes. To test this hypothesis, cells were allowed to internalize two consecutive pulses of transferrin, the first (rhodamine-labelled transferrin) for 1 h and the second (Alexa-488-labelled transferrin) for 15 min. In

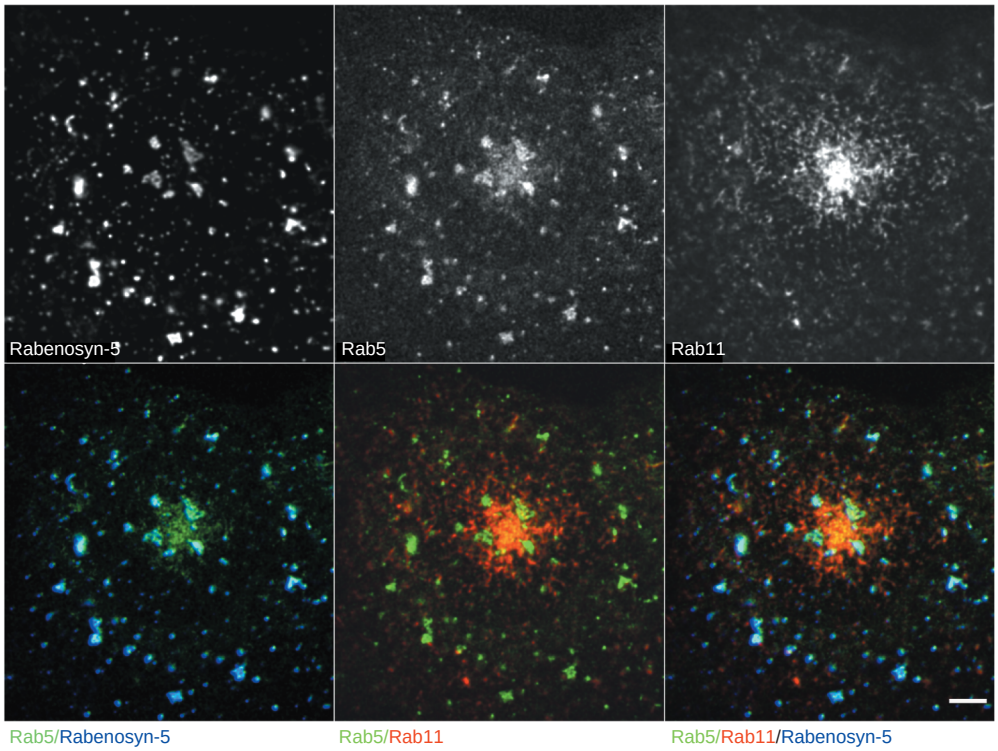

Figure 6 **Rabenosyn-5 overexpression does not change the perinuclear localization of Rab11-positive membranes.** A431 cells expressing CFP–Rab5, YFP–Rab11 and Rabenosyn-5 were fixed and stained with an anti-Rabenosyn-5 affinity-purified antibody and with Texas-Red-conjugated secondary antibodies. Individual confocal sections are shown. Scale bar, 5 μm.

control cells (Fig. 7f–h), both rhodamine- and Alexa-488-labelled transferrin colocalized into perinuclear recycling endosomes. Peripheral structures labelled either by Alexa-488–transferrin or by rhodamine–transferrin were also observed. By contrast, recycling endosomes were not labelled after 15 min of transferrin uptake into cells overexpressing Rabenosyn-5, (Fig. 7i). Only after 1 h of internalization could labelling of perinuclear recycling endosomes be observed (Fig. 7j). However, by comparison with control cells (Fig. 7h), the colocalization between the two consecutively internalized transferrin pulses in Rabenosyn-5-overexpressing cells was restricted to the peripheral enlarged structures (Fig. 7k). Therefore, these results suggest that Rabenosyn-5 overexpression promotes the recycling of transferrin directly from early endosomes and diminishes transport to perinuclear recycling endosomes.

To substantiate this conclusion, we measured the kinetics of transferrin recycling in cells overexpressing Rabenosyn-5. First, Rabenosyn-5 overexpression induced a moderate but significant increase in the steady state distribution of transferrin receptor on the plasma membrane (35% on the surface versus 25% in controls, data not shown). Second, to test whether the overall efficiency of the recycling pathway was perturbed, cells were labelled to steady state by internalizing biotinylated transferrin for 1 h at 37 °C. Surface-bound ligand was removed by ice-cold acid washes and recycling was restored by switching the temperature back to 37 °C. The amount of transferrin recycled into the medium was quantified. Overexpression of Rabenosyn-5 did not alter the total amount of recycled cargo, but instead accelerated the initial rate of recycling (Fig. 8a). The stimulation of recycling was even more evident after a short pulse (2 min) of transferrin internalization at 37 °C. Under these conditions, overexpression of Rabenosyn-5, but not of Rabenosyn-5δ, induced a ~3–4-fold stimulation of transferrin recycling (Fig. 8b). The stimulation was particularly evident in the first 4 min of the cycle, which corresponds to a $t_{1/2}$ of transferrin recycling of less than or equal to 3 min. Third, to synchronize recycling from early endosomes, transfected cells were allowed to internalize biotinylated-transferrin for 1 h at 16 °C. At this temperature, the transferrin receptor is efficiently internalized into early endosomes, but subsequent exit, either to recycling endosomes or to the cell surface, is impeded[34]. Consistent with the results of Fig. 7, Rabenosyn-5 overexpression significantly stimulated transferrin recycling during the first 5 min (Fig. 8c) without affecting the total amount of recycling at later time points (data not shown). Significantly, this increase was dependent on the Rabenosyn-5–Rab4 interaction, as overexpression of the Rabenosyn-5δ mutant failed to stimulate recycling and coexpression of the Rab4 dominant-negative mutant (Rab4S22N) neutralized this stimulation.

Finally, we tested whether Rabenosyn-5 overexpression also affects another stage of endocytic transport, that is, from early endosomes to late endosomes and lysosomes. To test this, we measured the rate of epidermal growth factor (EGF) degradation and found only a moderate kinetic delay (30% inhibition during the first 20 min; see Fig. 8d). Like the transferrin receptor, the EGF receptor may also be more efficiently recycled to the cell surface. Nevertheless, these results indicate that Rabenosyn-5 overexpression does not block transport to late endosomes and lysosomes.

Discussion

The sequential transport of cargo through membrane domains selectively occupied by Rab proteins implies that mechanisms exist to coordinate neighbouring domains, and to dictate the timing and specificity of each coupling event. Our data suggest that Rabenosyn-5, in conjunction with Rabaptin-5, regulates the functional link between Rab5 and Rab4 domains, and thus the transition of cargo between them. The finding that overexpression of Rabenosyn-5 modifies the distribution of Rab5, Rab4 and Rab11

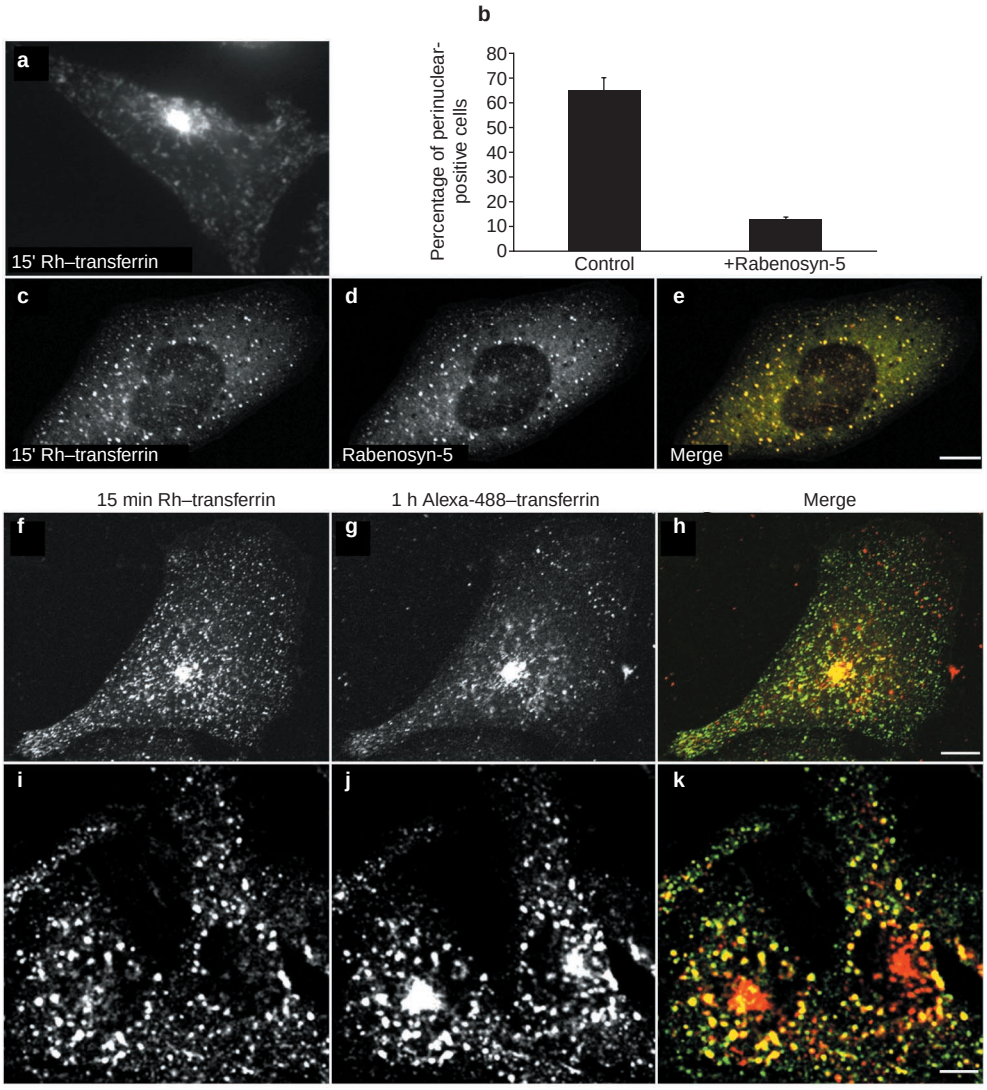

Figure 7 **Morphological analysis of transferrin transport. a**, **c–h**, Untransfected CHO cells (**a**) and CHO cells overexpressing Rabenosyn-5 (**c–e**) were incubated with 30 μg ml^{-1} of rhodamine–transferrin for 15 min at 37 °C. After extensive washing, cells were fixed and stained with anti-Rabenosyn-5 antibodies and then with Alexa-488-conjugated secondary antibodies. Individual confocal sections are shown. **b**, Percentage of cells showing labelling of perinuclear recycling endosomes after 15 min of rhodamine–transferrin uptake ($n = 200$). **f–k**, Untransfected CHO cells (**f–h**) or CHO cells overexpressing Rabenosyn-5 (**i–k**) were allowed to internalize two consecutive pulses of transferrin. Rhodamine–transferrin was internalized for 1 h and Alexa-488–transferrin for 15 min. Individual confocal sections are shown. Scale bar is 4 μm.

domains suggest that not only can early endosomes undergo homotypic fusion reactions *in vitro*[35] and *in vivo*[36,37], but that they can also dynamically re-arrange their subcompartmental organization.

First, Rabenosyn-5 must be recruited to the Rab5-positive domain, as the presence of Rabenosyn-5 was undetectable on structures positive for Rab4 alone (Fig. 3). As Rab5 and Rab4 have similar affinities for Rabenosyn-5 (Fig. 2d), we suggest that the targeting of the protein, like EEA1 (ref. 17), is dependent on the concomitant presence of Rab5 and PI(3)P[18]. Furthermore, the Rab4-binding domain of Rabaptin-5 is insufficient to recruit Rabaptin-5 to early endosomes[30]. Consistent with the membrane-tethering function of Rab effectors[13,28,29,38,39], Rabenosyn-5 may tether Rab5- and Rab4-containing membranes together. Rabenosyn-5 is complexed to the Sec1-related protein hVps45, a protein that interacts with various syntaxins (syntaxin4, 6 and 13) of the early endocytic pathway[18]. It is easy to imagine that the Rabenosyn-5–hVps45 complex could provide a regulatory function for the pairing of SNAREs after Rab5–Rab4 membrane tethering and/or during recycling from early endosomes to the plasma membrane[40,41]. Another possibility is that Rabenosyn-5 stimulates homotypic fusion between Rab5–Rab5 and Rab4–Rab4 domains. However, although this is possible for Rab5 (ref. 18), it seems unlikely in the case of the Rab4 domain which, when uncoupled from Rab5, harbours no detectable Rabenosyn-5. Furthermore, instead of the expected equal increase in Rab5–Rab4- and Rab4–Rab11-positive structures, Rabenosyn-5 overexpression caused Rab4 to shift from Rab11- to Rab5-positive structures (Table 1). A third possibility is that if Rab5- and Rab4-positive domains are in dynamic equilibrium between fusion and fission events, Rabenosyn-5 and Rabaptin-5 may stabilize the connection between the two domains and counteract fission. They may also confer a specific structural configuration to the junction between endosomal subcompartments (for example, by connecting vacuoles and tubules).

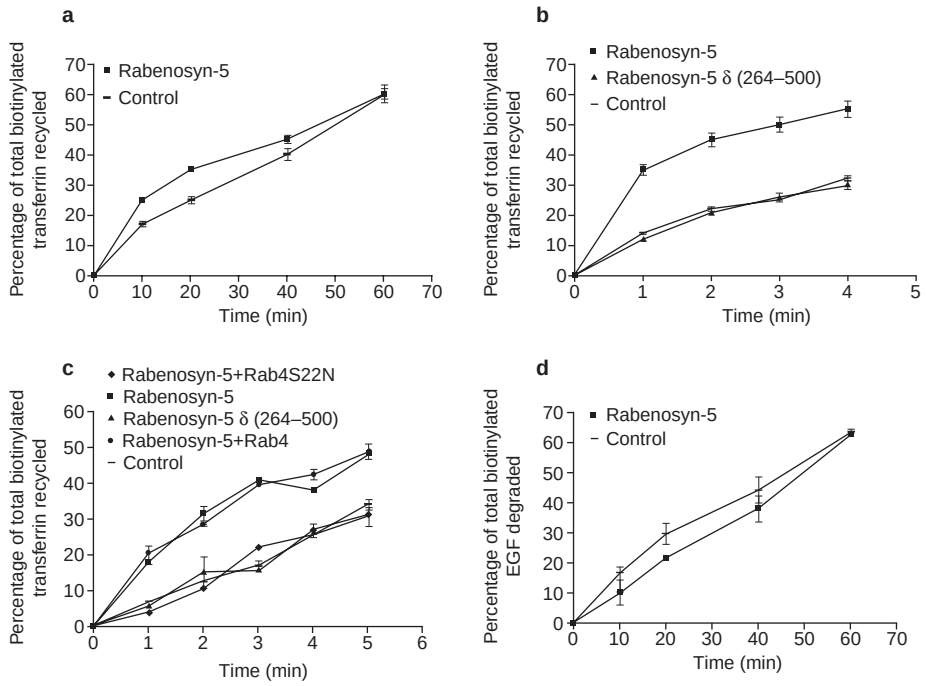

Figure 8 **Effects of Rabenosyn-5 overexpression on transferrin recycling and EGF degradation. a–c**, HeLa cells were transfected with the indicated plasmids and then infected with recombinant T7 RNA polymerase vaccinia virus. Cells were allowed to internalize biotinylated transferrin (10 μg ml^{-1}) at 37 °C for 1 h (**a**), 2 min (**b**), or 1 h at 16 °C (**c**). Cells were washed, stripped of surface-bound transferrin, and incubated at 37 °C in medium containing unlabelled transferrin. The amount of biotinylated transferrin released into the medium was monitored at the indicated times. Results are expressed as percentage of recycled biotinylated transferrin (ratio between marker in the medium/total marker. Total marker = marker in medium + intracellular marker). **d**, HeLa cells were transfected and infected with vaccinia virus, as in **a**, and the amount of biotinylated-EGF degradation was estimated, as described in the Methods.

Our data suggest that several molecular requirements must first be fulfilled for a physical connection between Rab5 and Rab4 domains to occur. We have determined that a key regulatory step of this process lies in the ability of Rabenosyn-5 to interact directly with Rab4 (Fig. 5). The distribution of Rab5- and Rab4-positive domains, together with the localization of Rabenosyn-5, implies that only a fraction of Rabenosyn-5 is bound to Rab4 at steady state. This interaction is dependent on several criteria. First, the interaction of Rabenosyn-5 and Rabaptin-5 requires GTP-bound Rab4 (Fig. 1). Rabaptin-5 is also part of a complex with Rabex-5 (ref. 14). The exchange activity of the Rabex-5 may ensure the activation of Rab5 at the Rab5–Rab4 junction, allowing the recruitment of Rabenosyn-5. Another goal is to identify which guanine nucleotide-exchange factor (GEF) activates Rab4. An interesting possibility is that Rabex-5 itself may also catalyse GDP/GTP exchange on Rab4. In this case, activation of Rab5 and recruitment of the Rabaptin–Rabex-5 complex would first be required before Rab4 could be activated. Second, Rabenosyn-5, as well as Rabaptin-5, seem to be rate-limiting components for the coupling between Rab5 and Rab4 domains. A single Rabenosyn-5 molecule is probably insufficient, and multiple Rabenosyn-5–Rab4 complexes may be required to bridge the Rab5- and Rab4-positive domains. This implies that the density of active Rab4 in the Rab4-positive domain is an important regulatory factor. However, Rab4 is also probably engaged in interactions with other Rab4 effectors, including Rabip4 (ref. 32). An exciting possibility raised by our findings is that some Rab4 effectors may regulate the association between Rab4 and Rab11 domains. Third, other Rabenosyn-5-interacting factors that have not yet been identified may participate in Rab5–Rab4 domain coupling.

There are two probable reasons why Rabenosyn-5 stimulates transferrin recycling. First, assuming that the transition from the Rab5- to the Rab4-positive domain is necessary for fast recycling, Rabenosyn-5 overexpression would stimulate this process by promoting the link between Rab5- and Rab4-positive domains (see Table 1). Second, by decreasing the coupling between Rab4- and Rab11-positive domains, an excess of Rabenosyn-5 would decrease the probability of transferrin receptor recycling through the slow route, and instead would increase recycling by the fast route. It is also possible that overexpression of Rabenosyn-5 may exert a negative effect on the regulation of transport between early endosomes and recycling endosomes. In this case it would activate the fast pathway and switch off the slow recycling route through Rab11-positive membranes.

In conclusion, the function of divalent Rab effectors, such as Rabenosyn-5, may define a new mechanism to regulate the structure, sorting and transport activities of the early endosomal compartment. In principle, this mechanism could also operate in the biosynthetic pathway. The activity of divalent Rab effectors should enhance our understanding of how recycling from early endosomes is regulated and perhaps clarify the, as yet, elusive function of recycling endosomes. □

Methods

Cell lines, antibodies and plasmids

A431 cells were grown in DMEM supplemented with 10% (v/v) heat-inactivated fetal calf serum, 100U ml^{-1} penicillin, 100 μg ml^{-1} streptomycin and 2 mM L-glutamine. Chinese hamster ovary (CHO) cells were cultured in Ham's F-12 medium supplemented with 10% (v/v) heat-inactivated fetal calf serum, 100U ml^{-1} penicillin, 100 μg ml^{-1} streptomycin. Polyclonal rabbit antibodies against Rabenosyn-5 (1:1000) were affinity purified, as previously described[18]. Polyclonal rabbit antibodies against Rabaptin-5, Rabaptin-5β, p110β and Rabex-5 (ref. 14) were used as crude serum at 1:1000 (western blotting) or 1:200 (immunofluorescence). Human anti-EEA1 serum (1:1000) was a gift from Ban Hok Toh (Monash Medical School, Adelaide, Australia). HRP- and fluorescently-labelled secondary antibody conjugates were purchased from Dianova (Hamburg, Germany). cDNAs encoding Rabenosyn-5, Rabaptin-5, EEA1, hVps45 and the human transferrin receptor (hTfR) were subcloned into the mammalian expression vector pcDNA3 (Clontech, Heidelberg, Germany). cDNAs encoding Rab4, Rab5 and Rab11 were fused to the amino termini of pECFP-C3 and pEYFP-C3 vectors (Clontech) or to pGEX (Pharmacia, Freiburg, Germany).

Sequential affinity chromatography

Rab5 effectors were purified as previously described[42]. Briefly, *Escherichia coli* DH5α cells (30 l) were grown to express GST–Rab5 and the protein was purified with 5 ml of glutathione beads, according to manufacturer's instructions (Pharmacia). Purified GST–Rab5 was then incubated with nucleotide-exchange buffer (buffer A) containing 20 mM HEPES, 100 mM sodium chloride, 10 mM EDTA, 5 mM magnesium chloride, 1 mM dithiothreitol and 1 mM GTPγS at pH 7.5, for 90 min at room temperature, under rotation. Buffer A was then removed and the GTPγS form of GST–Rab5 was stabilized with buffer B, containing 20 mM HEPES, 100 mM sodium chloride, 5 mM magnesium chloride and 1 mM dithiothreitol at pH 7.5, in the presence of 1 mM GTPγS for 20 min at room temperature, under rotation. Beads were then incubated for 120 min at 4 °C with bovine brain cytosol prepared as before[42]. Beads were washed with ten column volumes of buffer B containing 10 μM GTPγS, ten column volumes of buffer B containing 250 mM sodium chloride (final concentration) and 10 μM GTPγS and one column volume of 20 mM HEPES, 250 mM sodium chloride and 1 mM dithiothreitol at pH 7.5. Bound proteins were eluted with 1.5 column volumes of buffer C, containing 20 mM HEPES, 1.5 M sodium chloride, 20 mM EDTA, 1 mM dithiothreitol and 5 mM GDP at pH 7.5, and incubated with the beads for 20 min at room temperature, under rotation. Eluted proteins were first treated twice with 0.2 ml glutathione Sepharose beads for 1 h at 4 °C to remove GST–Rab5 which leaked from the affinity column during the elution step. The sample was then desalted with PD10 columns (Pharmacia) in a nucleotide-free buffer containing 20 mM HEPES, 150 mM sodium chloride and 1 mM dithiothreitol at pH 7.5. The Rab5-interacting proteins obtained by this method were then incubated with 1 ml of glutathione beads containing GST–Rab4 loaded with either GTPγS, or GDP as a control. GST–Rab4 was prepared as described for GST–Rab5. To generate the GDP form of GST–Rab4, the following changes were made: all buffers contained GDP instead of GTPγS, except for the elution buffer which contained GTPγS (1 mM) instead of GDP. Bound proteins were eluted with buffer C, separated by SDS–PAGE and analysed by western blot or mass spectroscopy.

In vitro binding assay and affinity measurement

Rabenosyn-5 and hVps45 cDNAs were *in vitro* transcribed and translated in the presence of ^{35}S-methionine, with the TnT coupled transcription-translation kit. Binding assays were performed as previously described[15], by incubating 50 μl of the translated proteins with 30 μl of GST–Rab5, GST–Rab4 or GST–Rab11, loaded with either GDP or GTPγS. Bound proteins were eluted, separated by SDS–PAGE and analysed by autoradiography.

For the binding experiment in insect cells, proteins were overexpressed by infecting cells with recombinant baculovirus carrying Rabenosyn-5 and hVps45 cDNAs, according to manufactories instructions (Life Technologies, Karlsruhe, Germany). To achieve optimal protein expression levels, 500 ml of suspension-grown ExpresSf+ insect cells (1×10^6 cells ml^{-1}; Protein Science, Meriden, CT) were infected at a multiplicity of infection of 2, and incubated for a further 52 h. Cells were harvested by centrifugation and cytosol prepared as previously described[14]. Approximately 8 mg of total proteins were incubated for 2 h at 4 °C with 100 μl beads containing ~400 μg GST–Rab4 loaded with GTPγS. After extensive washes with buffer B, beads were further incubated for 1 h with ~200 μg of purified Rab5-GTPγS and 10 mg ml^{-1} BSA diluted in buffer B. Beads were washed with 10 ml of buffer B and bound proteins eluted as described above.

The K_d values of the Rab5–Rabenosyn-5 and Rab4–Rabenosyn-5 interactions were determined by a previously described method to measure the affinity between tau proteins and tubuline[43]. Briefly, Rabenosyn-5 was *in vitro* translated in the presence of ^{35}S-methionine with the TnT coupled transcription-translation kit. The translated protein (20 μl) was incubated at room temperature for 1 h with serial dilutions of glutathione–Sepharose beads containing GST–Rab4 or GST–Rab5 in 200 μl of buffer B (with the total amount of Rabenosyn-5 always well below the concentration of GST–Rab, to ensure maximal binding). Beads were spun through a 40% sucrose cushion (1 ml) to separate bound from unbound Rabenosyn-5. Proportional aliquots of bound, unbound and total-loaded fractions were separated by SDS–PAGE and analysed with a phosphoimager reader for quantification. Binding of Rabenosyn-5 to empty GST beads was considered to be background, and therefore subtracted from each binding value before calculating the binding percentage.

Internalization of fluorescently labelled transferrin, immunofluorescence and microinjection

In order to study the effects of Rabenosyn-5 overexpression on the endosomal localization of Rab proteins, appropriate plasmids were injected into the nucleus of A431 cells with an Eppendorf micromanipulator and transjector. The expression level of CFP fusion proteins was generally lower than that of YFP fusion proteins. A mixture of 7 ng μl^{-1} YFP, 20 ng μl^{-1} CFP and 50 ng μl^{-1} Rabenosyn-5, Rabaptin-5 or EEA1 plasmid cDNAs were chosen as a standard concentration in all microinjection experiments. Immunofluorescence labelling was performed according to standard procedures. Cells were mounted in ProLong Antifade (Molecular Probes, Leiden, Netherlands).

CHO cells were grown on glass coverslips (MatTek Corp., Ashland, MA) and microinjected with 50 ng μl^{-1} of appropriate plasmid, as described above. After 24 h, cells were serum starved for 1 h before incubation with 30 μg ml^{-1} of rhodamine-labelled transferrin, or Alexa-488-labelled transferrin (Molecular Probes).

Confocal microscopy, image processing and quantification of signal overlap on fixed cells

Confocal microscopy was performed on the compact confocal camera (CCC), as previously described[20]. For multichannel imaging, fluorescent dyes were imaged sequentially in either frame-interlace or line-interlace modes, to eliminate cross talk between the channels. CFP was excited with a 430-nm laser line (Directly Doubled Diode/D3, Coherent, Santa Clara, CA) and imaged through a combination of 440–505-nm bandpass and 525-nm longpass emission filters. YFP was exited with a 514-nm argon laser line and imaged through a 525-nm longpass emission filter. Texas Red was excited with a 594-nm helium–neon laser line and imaged through a 610-nm longpass emission filter.

Serial sections of images were acquired and satisfied the Nyquist criteria for sampling. Images were then processed on a multiprocessor SGI Unix computer, with the Huygens System 2.2 (Scientific Volume Imaging BV, Netherlands). A maximum likelihood estimation (MLE)-based algorithm was used for image reconstruction. *Z*-stacks of images were exported as TIFF files, and individual sections were analysed for fluorescent signal overlap by visual inspection. A 5 cm^2 grid was projected onto the image of the reference channel (for example Texas-Red–transferrin) with Adobe Photoshop 5 software. In every second grid square, all fluorescent structures were marked on a separate, superimposed layer. Signals were referred to as individual structures if they comprised a continuous patch of intensity values above 50 (in a range of 0–255). This layer was then projected onto the corresponding images for the other two channels (for example YFP–Rab4 and CFP–Rab5), and the underlying image was analysed for fluorescent signal at the marked position. At least two sections per cell were counted, ensuring that peripheral and perinuclear structures were taken into account equally.

Kinetic analysis of transferrin recycling and EGF degradation

For T7-promoter-driven overexpression experiments, HeLa cells were grown to 60% confluence, transfected with the appropriate plasmids and infected with T7 polymerase recombinant vaccinia virus, as previously described[36]. After 4 h, infected cells were washed twice with PBS and biotinylated transferrin (10 μg ml^{-1}) was internalized for the indicated times. Unbound and surface-bound transferrin was removed by washing the cells with ice-cold PBS containing 1 mg ml^{-1} transferrin and then by cold low-pH buffer washes (150 mM sodium chloride, 10 mM acetic acid at pH 3.5 and 1 mg ml^{-1} transferrin). This procedure was repeated twice, resulting in the removal of 95–98% of surface-bound ligand (from cells that had been incubated with biotinylated transferrin for 1 h on ice). To measure recycling, cells were returned to 37 °C and incubated in 1 ml of medium containing unlabelled transferrin (1 mg ml^{-1}). At each time point, an aliquot of medium was collected. At the end of the time course, cells were washed twice with ice-cold PBS and homogenized in 1 ml of lysis buffer (PBS containing 2% Triton-X100, 0.4% SDS). A proportion of the collected medium (30 μl) containing the recycled biotinylated transferrin, or the lysate (30 μl) containing the cell-associated biotinylated transferrin, were quantified as described previously[44]. For each time point, results were expressed as a percentage of the total signal.

EGF transport was analysed by internalization of a biotinylated EGF 'pulse' (1 nM) for 5 min at 37 °C, extensive washing and a 'chase' at the same temperature for the indicated times. EGF degradation was estimated by quantifying the amount of biotinylated EGF accessible to an anti-EGF antibody, with the same electrochemiluminescence detection system used to quantify biotinylated transferrin recycling.

RECEIVED 17 JANUARY 2001; REVISED 12 NOVEMBER 2001; ACCEPTED 12 NOVEMBER 2001; PUBLISHED 14 JANUARY 2002.

1. Mukherjee, S., Ghosh, R. N. & Maxfield, F. R. Endocytosis. *Physiol. Rev.* **77,** 759–803 (1997).
2. Dunn, K. W., McGraw, T. E. & Maxfield, F. R. Iterative fractionation of recycling receptors from lysosomally destined ligands in an early sorting endosome. *J. Cell Biol.* **109,** 3303–3314 (1989).
3. Hopkins, C. R. Intracellular routing of transferrin and transferrin receptors in epidermoid carcinoma A431 cells. *Cell* **35,** 321–330 (1983).
4. Mayor, S., Presley, J. F. & Maxfield, F. R. Sorting of membrane components from endosomes and subsequent recycling to the cell surface occurs by a bulk flow process. *J. Cell Biol.* **121,** 1257–1269 (1993).
5. Mellman, I. Endocytosis and molecular sorting. *Annu. Rev. Cell Dev. Biol.* **12,** 575–625 (1996).
6. Gruenberg, J. & Maxfield, F. R. Membrane transport in the endocytic pathway. *Curr. Opin. Cell Biol.* **7,** 552–563 (1995).
7. Rohn, W. M., Rouille, Y., Waguri, S. & Hoflack, B. Bi-directional trafficking between the *trans*-Golgi network and the endosomal/lysosomal system. *J. Cell Sci.* **113,** 2093–2101 (2000).
8. Wilcke, M. *et al.* Rab11 regulates the compartmentalization of early endosomes required for efficient transport from early endosomes to the *trans*-Golgi network. *J. Cell Biol.* **151,** 1207–1220 (2000).
9. Schmid, S. L., Fuchs, R., Male, P. & Mellman, I. Two distinct subpopulations of endosomes involved in membrane recycling and transport to lysosomes. *Cell* **52,** 73–83 (1988).
10. Yamashiro, D. J., Tycko, B., Fluss, S. R. & Maxfield, F. R. Segregation of transferrin to a mildly acidic (pH 6.5) *para*-Golgi compartment in the recycling pathway. *Cell* **37,** 789–800 (1984).
11. Zerial, M. & McBride, H. Rab proteins as membrane organizers. *Nature Rev. Mol. Cell Biol.* **2,** 107–117 (2001).
12. Miaczynska, M. & Zerial, M. Mosaic organization of the endocytic pathway. *Exp. Cell Res.* **272,** 8–14 (2002).
13. Christoforidis, S., McBride, H. M., Burgoyne, R. D. & Zerial, M. The Rab5 effector EEA1 is a core component of endosome docking. *Nature* **397,** 621–625 (1999).
14. Horiuchi, H. *et al.* A novel Rab5 GDP/GTP exchange factor complexed to Rabaptin-5 links nucleotide exchange to effector recruitment and function. *Cell* **90,** 1149–1159 (1997).
15. Christoforidis, S. *et al.* Phosphatidylinositol-3-OH kinases are Rab5 effectors. *Nature Cell Biol.* **1,** 249–252 (1999).
16. Schu, P. V. *et al.* Phosphatidylinositol 3-kinase encoded by yeast VPS34 gene essential for protein sorting. *Science* **260,** 88–91 (1993).
17. Simonsen, A. *et al.* EEA1 links PI(3)K function to Rab5 regulation of endosome fusion. *Nature* **394,** 494–498 (1998).
18. Nielsen, E. *et al.* Rabenosyn-5, a novel rab5 effector, is complexed with hVPS45 and recruited to endosomes through a FYVE finger domain. *J. Cell Biol.* **151,** 601–612 (2000).
19. Simonsen, A., Gaullier, J. M., D'Arrigo, A. & Stenmark, H. The Rab5 effector EEA1 interacts directly with syntaxin-6. *J. Biol. Chem.* **274,** 28857–28860 (1999).
20. Sonnichsen, B., De Renzis, S., Nielsen, E., Rietdorf, J. & Zerial, M. Distinct membrane domains on endosomes in the recycling pathway visualized by multicolor imaging of Rab4, Rab5, and Rab11. *J. Cell Biol.* **149,** 901–914 (2000).
21. McBride, H. M. *et al.* Oligomeric complexes link Rab5 effectors with NSF and drive membrane fusion via interactions between EEA1 and syntaxin 13. *Cell* **98,** 377–386 (1999).
22. van der Sluijs, P. *et al.* The small GTP-binding protein rab4 controls an early sorting event on the endocytic pathway. *Cell* **70,** 729–740 (1992).
23. Ullrich, O., Reinsch, S., Urbe, S., Zerial, M. & Parton, R. G. Rab11 regulates recycling through the pericentriolar recycling endosome. *J. Cell Biol.* **135,** 913–924 (1996).
24. Geuze, H. J., Slot, J. W., Strous, G. J. & Schwartz, A. L. The pathway of the asialoglycoprotein-ligand during receptor-mediated endocytosis: a morphological study with colloidal gold/ligand in the human hepatoma cell line, Hep G2. *Eur. J. Cell Biol.* **32,** 38–44 (1983).
25. Griffiths, G., Back, R. & Marsh, M. A quantitative analysis of the endocytic pathway in baby hamster kidney cells. *J. Cell Biol.* **109,** 2703–2720 (1989).

26. Clague, M. J. Membrane transport: Take your fusion partners. *Curr. Biol.* **9,** R258–R260 (1999).
27. VanRheenen, S. M., Cao, X., Lupashin, V. V., Barlowe, C. & Waters, M. G. Sec35p, a novel peripheral membrane protein, is required for ER to Golgi vesicle docking. *J. Cell Biol.* **141,** 1107–1119 (1998).
28. Cao, X., Ballew, N. & Barlowe, C. Initial docking of ER-derived vesicles requires Uso1p and Ypt1p but is independent of SNARE proteins. *EMBO J.* **17,** 2156–2165 (1998).
29. Allan, B. B., Moyer, B. D. & Balch, W. E. Rab1 recruitment of p115 into a *cis*-SNARE complex: programming budding COPII vesicles for fusion. *Science* **289,** 444–448 (2000).
30. Vitale, G. *et al.* Distinct Rab-binding domains mediate the interaction of Rabaptin-5 with GTP-bound Rab4 and Rab5. *EMBO J.* **17,** 1941–1951 (1998).
31. Burd, C. G., Peterson, M., Cowles, C. R. & Emr, S. D. A novel Sec18p/NSF-dependent complex required for Golgi-to-endosome transport in yeast. *Mol. Biol. Cell* **8,** 1089–1104 (1997).
32. Cormont, M., Mari, M., Galmiche, A., Hofman, P. & Le Marchand-Brustel, Y. A FYVE-finger-containing protein, Rabip4, is a Rab4 effector involved in early endosomal traffic. *Proc. Natl Acad. Sci. USA* **98,** 1637–1642 (2001).
33. Daro, E., van der Sluijs, P., Galli, T. & Mellman, I. Rab4 and cellubrevin define different early endosome populations on the pathway of transferrin receptor recycling. *Proc. Natl Acad. Sci. USA* **93,** 9559–9564 (1996).
34. Sipe, D. M., Jesurum, A. & Murphy, R. F. Absence of Na^+-K^+-ATPase regulation of endosomal acidification in K562 erythroleukemia cells. Analysis via inhibition of transferrin recycling by low temperatures. *J. Biol. Chem.* **266,** 3469–3474 (1991).
35. Gorvel, J. P., Chavrier, P., Zerial, M. & Gruenberg, J. Rab5 controls early endosome fusion *in vitro*. *Cell* **64,** 915–925 (1991).
36. Bucci, C. *et al.* The small GTPase rab5 functions as a regulatory factor in the early endocytic pathway. *Cell* **70,** 715–728 (1992).
37. Murphy, C. *et al.* Endosome dynamics regulated by a Rho protein. *Nature* **384,** 427–432 (1996).
38. Guo, W., Roth, D., Walch-Solimena, C. & Novick, P. The exocyst is an effector for Sec4p, targeting secretory vesicles to sites of exocytosis. *EMBO J.* **18,** 1071–1080 (1999).
39. Price, A., Seals, D., Wickner, W. & Ungermann, C. The docking stage of yeast vacuole fusion requires the transfer of proteins from a *cis*-SNARE complex to a Rab/Ypt protein. *J. Cell. Biol.* **148,** 1231–1238 (2000).
40. Olson, A. L., Knight, J. B. & Pessin, J. E. Syntaxin 4, VAMP2, and/or VAMP3/cellubrevin are functional target membrane and vesicle SNAP receptors for insulin-stimulated GLUT4 translocation in adipocytes. *Mol. Cell Biol.* **17,** 2425–2435 (1997).
41. Prekeris, R., Klumperman, J., Chen, Y. A. & Scheller, R. H. Syntaxin 13 mediates cycling of plasma membrane proteins via tubulovesicular recycling endosomes. *J. Cell Biol.* **143,** 957–971 (1998).
42. Christoforidis, S. & Zerial, M. Purification and identification of novel Rab effectors using affinity chromatography. *Methods* **20,** 403–410 (2000).
43. Butner, K. A. & Kirschner, M. W. Tau protein binds to microtubules through a flexible array of distributed weak sites. *J. Cell Biol.* **115,** 717–730 (1991).
44. Zacchi, P. *et al.* Rab17 regulates membrane trafficking through apical recycling endosomes in polarized epithelial cells. *J. Cell Biol.* **140,** 1039–1053 (1998).

ACKNOWLEDGEMENTS
We are grateful to E. Nielsen, for many constructive comments and advice at the beginning of the project, and for anti-Rabenosyn-5 antibodies. We also thank A. Runge for technical assistance and B. Hoflack, H. McBride and K. Simons for critical reading of the manuscript and helpful comments. This work was supported by the Max Planck Society and by grants from Human Frontier Science Program (RG-0260/1999), European Union 5th Framework Programme (HPRN-CT-2000-00081) and Biomed (BMH4-97-2410) to M.Z.
Correspondence and requests for material should be addressed to M.Z.